American Scientific Research Journal for Engineering, Technology, and Sciences (ASRJETS)
ISSN (Print) 2313-4410, ISSN (Online) 2313-4402

http://asrjetsjournal.org/

Study of an Injection on the Mamwe Comoros Network of Solar Photovoltaic Energy through a Static Switch

Said Mohamed Mariama[a*], Angel Scipioni[b], Bernard Davat[c]

[a,b]*Université de Lorraine, Groupe de Recherche en Electrotechnique et Electronique de Longwy (GREEN), 186, rue de Lorraine 54400 Cosnes et Romain, France*

[c]*Université de Lorraine, Groupe de Recherche en Electrotechnique et Electronique de Nancy (GREEN), 2, avenue de la forêt de Haye 54518 Vandoeuvre lès Nancy, France*

[a]*Email: mariamasaidmohamed@gmail.com*

[b]*Email: angel.scipioni@univ-lorraine.fr*

[c]*Email: Bernard.davat@univ-lorraine.fr*

Abstract

This article proposes to study the injection of photovoltaic solar energy into the network through a current switch. In this work, we opted for the implementation of a solar energy injection device in the network through a thyristor current switch given the property offered by this type of component to easily allow switching at high power. However, like any static switch, this type of component inevitably leads to a deterioration of the quality of the current and the voltage in the distribution networks. The simulation results made it possible to determine the behavior of the energy chain with respect to variations of the sun, the reactive component, the harmonics and their compensation.

Keywords: photovoltaic generator; current switch; network.

1. Introduction

The photovoltaic system market [1, 2-3] has been experiencing very high growth over the last decade. According to the Photovoltaic (PV) Market Alliance (recent report of 15th June, 2016) global PV markets should reach at least 60 GW in 2016 and more than 70 GW in 2017[4].

---

* Corresponding author.

This continuous growth, especially for systems connected to the electricity distribution network [5, 6,7-8], is due to numerous technological innovations, to the lowering of the costs of photovoltaic modules [9, 10], to a feed-in tariff for photovoltaic kWh at a very attractive price in some countries for the production of electricity from renewable sources and the reduction of greenhouse gas emissions [11,12]. The idea of a study of the photovoltaic sector connected to the Comoros power grid is a real national challenge when we know the state of energy poverty. For several years now, the Comorian authorities have initiated a profound reform in the energy sector aimed at ensuring sustainable development of the country, in particular by strengthening the role of Renewable Energies. The connection to the distribution network of photovoltaic systems necessarily involves the use of inverters. It is also through the control of their management that the quality of the supplied network energy will be improved. This aspect is also to be considered and will be developed later. It should be noted also the influence that this parameter has on the overall electricity production and thus on the profitability of a photovoltaic system.

2. System description

The block diagram of Figure 1 consists of three parts: the photovoltaic generator, the three-phase current switch and the three-phase network. We will briefly present a few related elements.

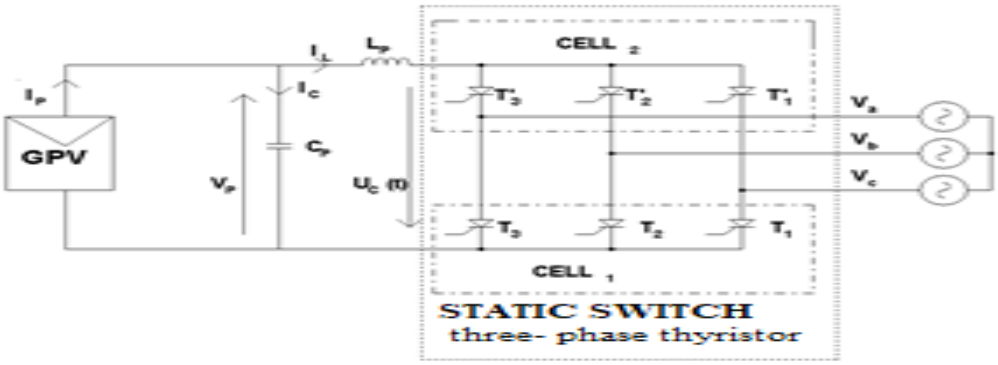

Figure 1: Diagram of the photovoltaic solar energy injection in the network through a static switch

In a three-phase switching device the average value of the voltage over a time interval T / 6 (T: Temperature of the junction in °K) is:

$$V_{cmoy} = \frac{6}{\pi}\int_{\theta-\frac{\pi}{6}}^{\theta+\frac{\pi}{6}} U_M \cos\omega t dt \qquad (1)$$

$$V_{cmoy} = \frac{3}{\pi}U_M \cos\theta = \frac{3}{\pi}\sqrt{6}V_a \cos\theta = V_{CM}\cos\theta \qquad (2)$$

(Where $V_{a:}$ RMS value of the single voltage of the three-phase source (V); U_M : Average voltage at the output of a three-phase inverter with thyristor bridge (V); V_{CM} : Value of the average maximum voltage (V)).

Average electrical power:

$$P_c = I_C V_{cmoy} = I_c \frac{3}{\pi}\sqrt{6} V_a \cos\theta = V_{CM} I_c \cos\theta \qquad (3)$$

(Where I_c: Current of the continuous source (A)).

The reactive power is given conventionally by:

$$Q = \frac{3\sqrt{6}}{\pi} V_a I_c \sin\theta \qquad (4)$$

3. Modeling of the photovoltaic generator

The photovoltaic generator (GPV) is modeled as a Multiple Inputs (MISO) system.

It is represented in FIG.2. The theoretical model of the PV generator is given by the relation:

$$I = \alpha I_{sc}\left(\frac{E_s}{1000}\right) - I_{sat}\left[exp\left\{\frac{e_0\left(\beta V + \frac{\beta R_s I}{\alpha}\right)}{\beta A K T}\right\} - 1\right] - \left(\frac{\beta V + \frac{\beta R_s I}{\alpha}}{\frac{\beta R_{sh}}{\alpha}}\right) \qquad (5)$$

(where I : Photovoltaic generator current (A); V : Voltage of the photovoltaic generators (V); E_S : Illuminance or global sunlight incident on the photovoltaic cell (W / m²); A :Ideal factor of the solar cell; R_{sh} : Parallel or shunt resistance (Ω); R_s : Rs: Resistance series of the photovoltaic cell (Ω); K : Boltzmann constant (1.3810e-23 J / K) Tref : Ambient temperature or cell junction; α : Number of associated photovoltaic modules in parallel; β: Number of associated photovoltaic modules in series).

The values of the simulation parameters are Es = 1000W/m²; T = 25 ° C.

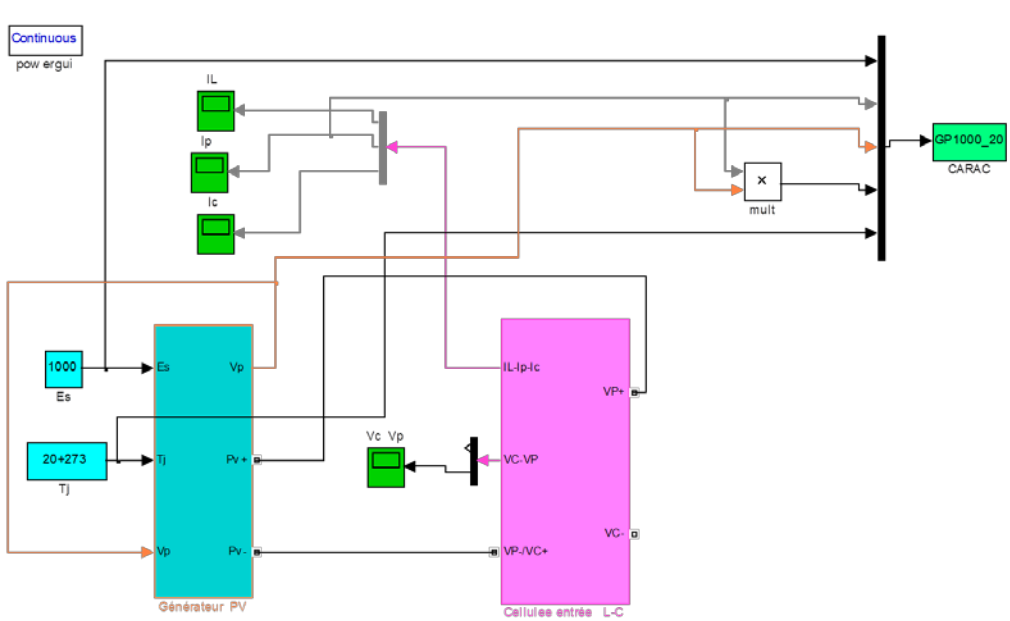

Figure 2: Photovoltaic generator block diagram

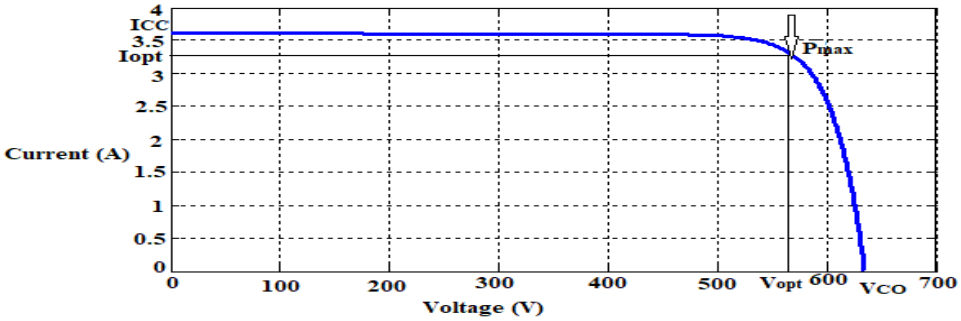

Figure 3: PV generator I-V characteristic

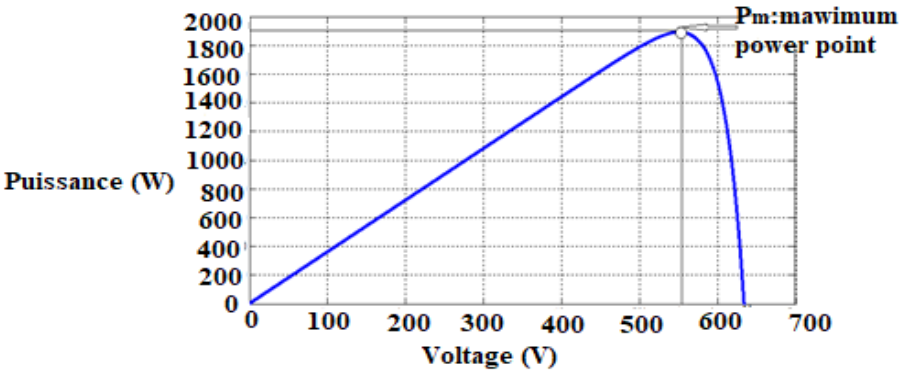

Figure 4: PV generator P-V characteristic

Figure 5 shows that the output current I of the GPV is significantly influenced by the change in insolation while the output voltage V remains approximately constant. However, for different values of the temperature, it can be seen that the open circuit voltage changes significantly while the short-circuit current is very little affected (Figure 6).

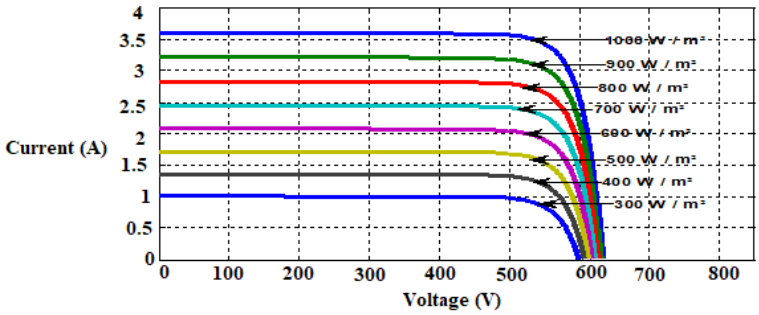

Figure 5: I-V current characteristic of the GPV for different sunlight values Es for a temperature of 25°C

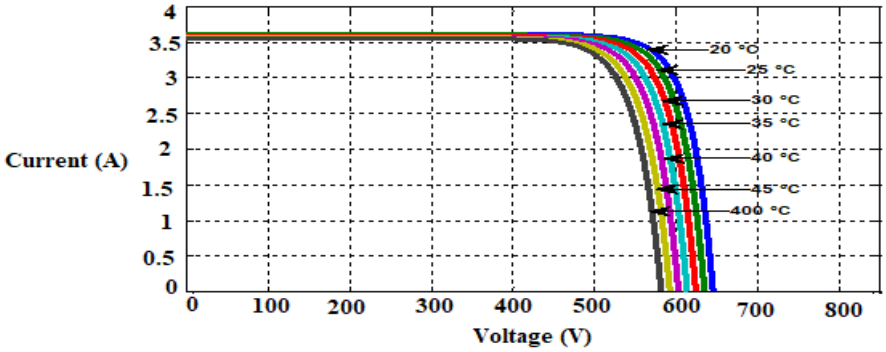

Figure 6: I-V characteristic of the GPV for different values of the temperature T at sunshine of 1000W / m²

The different simulation results show that the operating points of the GPV for an optimal transfer of the available power, define a privileged operating domain which will be the subject of constant attention thanks to a dedicated algorithm (MPPT).

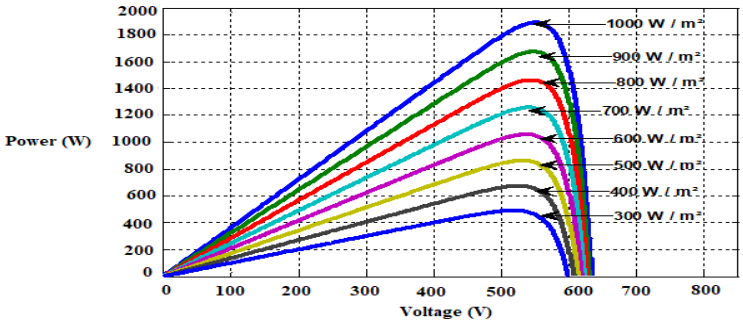

Figure 7: P-V characteristic of the GPV for different sunlight values Es at a temperature of 25 °C

Figure 7 confirms the expected behavior of a device that converts solar energy into electrical energy: the optimal output power of the GPV is significantly reduced for decreasing insolation. It also shows how the output power is reduced by increasing the temperature of the GPV.

This can be explained by the significant dependence of the temperature on the open circuit voltage, Vco, and the negative nature of the silicon temperature coefficient. It can also be noted that the output power of the GPV does not depend solely on the temperature and the insolation, but also on the operating voltage V (therefore of the load). This last element will be analyzed more particularly in the rest of the article. The point of the curve giving the maximum power P_m is called the maximum power point (MPP). By definition, Pm becomes the power delivered by the generator if it runs at its nominal load.

Figure 7 allowed us to determine the value of the maximum power of the photovoltaic generator. This value is of the order of 1,888 kW for sunshine of 1kW / m² at the temperature of 25 ° C (standard conditions).

This maximum power logically decreases with the weakening of sunshine. It goes from 1,461 kW for sunshine of 0.8 kW / m² to 0.464 kW for sunshine of 0.3 kW / m².

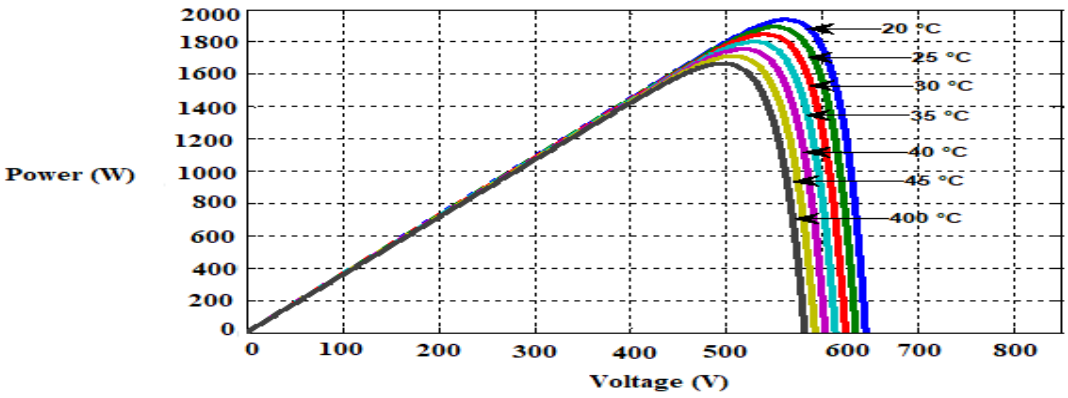

Figure 8: I-V characteristic of the GPV for different values of the temperature T at sunshine of 1000W/ m²

4. Injection of solar PV energy in the Comoros electricity network through a static switch

This part of the study deals with PV solar power injection into the network through a three-phase current switch. The GPV is connected to a capacitive DC bus, which gives the system as a whole a voltage source characteristic.

Since the current switch is connected to the three-phase electrical network (source of AC voltages), the character of the source on the DC side of the switch must be that of a source of the most stable current possible. which is obtained by associating in series with the whole GPV-continuous bus an inductance.

4.1. Behavior of the model of the energy chain GPV-Current switch-electrical network

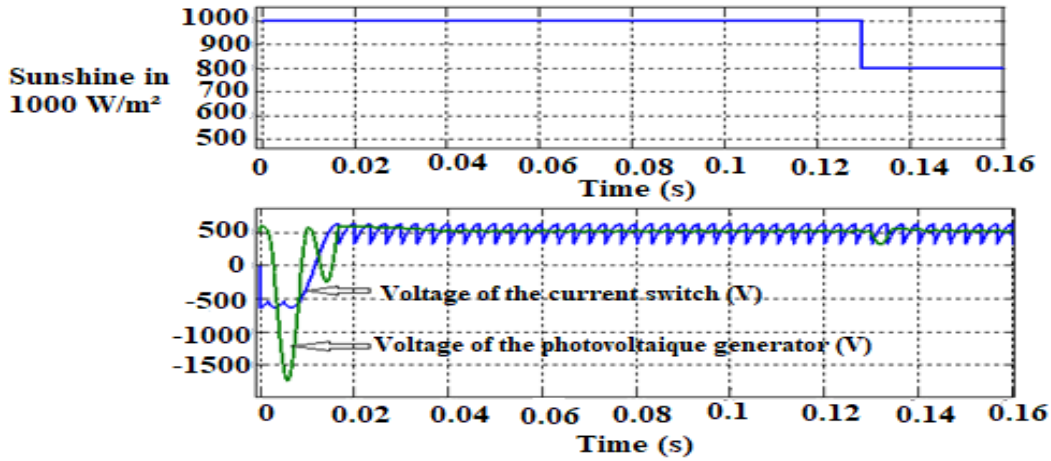

Figure 9: Behavior of the GPV voltages and Switch for a sudden change in sunshine

Figure 9 shows the behavior of the GPV-switch-sector chain when powering up and for the application of a sunshine step. We note that for about 20 ms, ie a period of mains voltages, the current switch operates in rectifier mode and not in inverter mode. This is because the control of the switch takes into account the composed voltages of the sector at the time of development of the commands. This implies that for a practical

implementation power on the power must be delayed by at least 20 ms. during these first 20 ms the voltage at the terminals of the GPV and consequently the power generated, are not controlled.

When a down step of sunshine ($\Delta Es = 200\ W/m^2$) occurs, the behavior of the energy chain is very satisfactory from the point of view of the variation of the amplitude of the disturbance, but is not without consequence from the harmonic point of view. Nevertheless, it can be seen in fig. 9, a readjustment of the voltage of the GPV on the average voltage of the switch after one sixth of the period of the mains voltages (therefore a period of the voltage on the DC side of the switch). This delay is structural and intrinc to the opertaion of the switch.

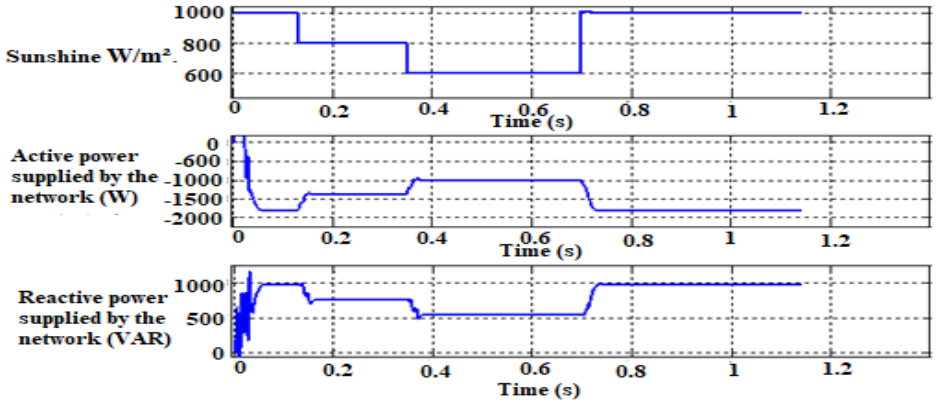

Figure 10: Active and Reactive power evolution at the current inverter

Figure 10 illustrates that logically the active power, P, and the reactive power in the network, Q, for a given command of the current inverter, evolve in the same direction as the sunshine. This is justified by analyzing the alternative magnitudes at the output of the power inverter. Indeed, these powers (active and reactive) are related only to two magnitudes: the simple effective sector voltages (V_{eff}) and the fundamental currents at the output of the current inverter (I_F). Keeping the control of the inverter constant will impose a constant phase shift (θ_F) between the voltage of a phase and the fundamental of its current. Moreover, since $P = 3 * V_{eff} * I_F * \cos(\theta_F)$ and $Q = 3 * V_{eff} * I_F * \sin(\theta_F)$ and because the mains voltage is considered constant, it can be concluded that these powers evolve proportionally with the effective value of the phase currents of the inverter. This last quantity being proportional to the current of the GPV which itself is proportional to the sunlight Es.

The load is a balanced effective voltage of 362V and three-phase system, figure 11.

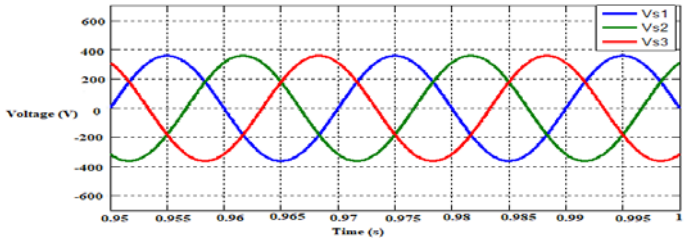

Figure 11: Voltages of the supply network

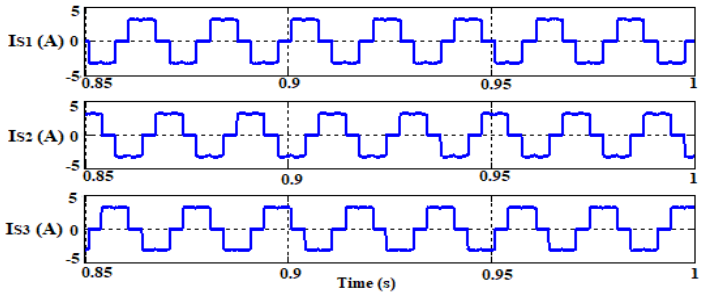

Figure 12: Current provided by the switch

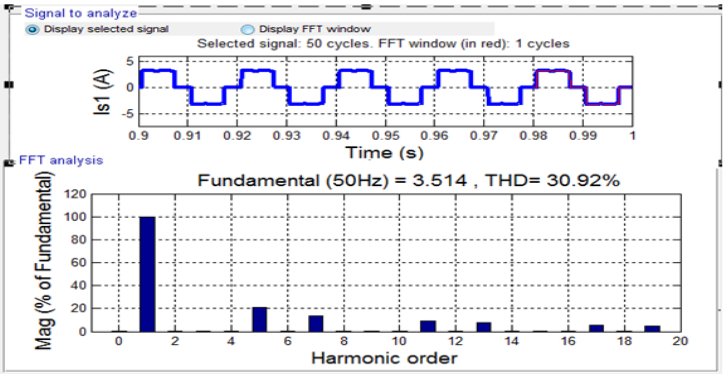

Figure 13: Current harmonic spectrum absorbed by the network

4.2. Operation with constant sunlight and variable inverter control

The sunshine is fixed and the ignition delay angle θ of the static switch is varied. For this purpose, we act on the V_{com} command, [such that θ = arc (V_{com})] which varies according to the values: [-0.504, -0.672, -0.88, -0.96, -1] (radians), for a temperature 25 ° C.

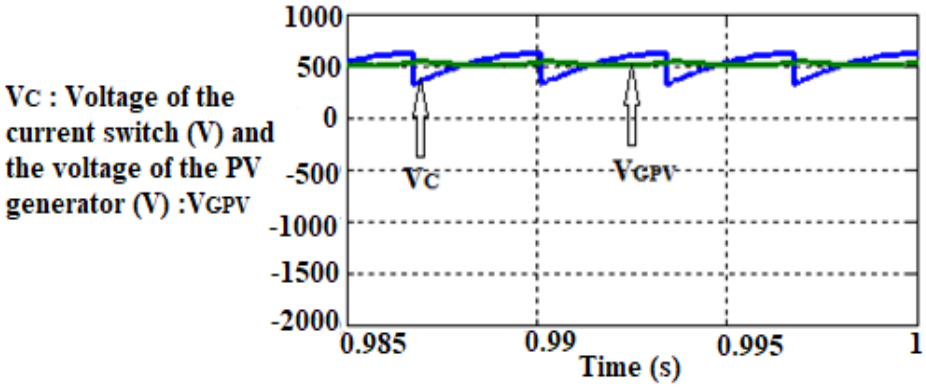

Figure 14: GPV voltage (green) and switch voltage (blue)

It can be seen in FIG. 14 that the voltage of the photovoltaic generator follows the mean value of the DC side voltage of the current switch.

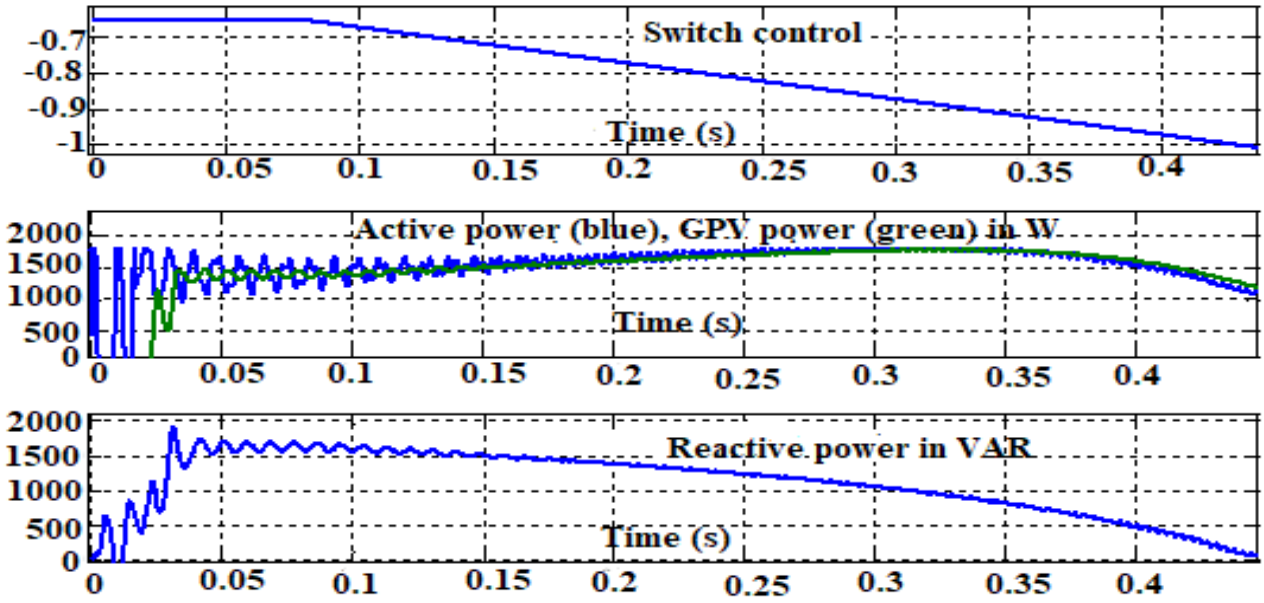

Figure 15: Evolution of active and reactive powers according to the order

By varying the V_{com} control, we find that the active power (P) absorbed by the power grid and that provided by the photovoltaic generator (P_{gpv}) are 1.8 kW (Figure 15). On the other hand the reactive power decreases until reaching the null value. It can be concluded that the electrical network provides reactive power as long as V_{com} is greater than -1, which corresponds to an angle $\theta < \pi$. Figure 15 also shows that the control of the current inverter optimizes the energy transfer from the photovoltaic generator. In Figure 15, corresponding to a solar irradiance of Es = 1 kW / m^2, we found a maximum power of the photovoltaic generator (GPV) of P_{gpv} = 1.800 W, for a command θ_{Vcom} = -0.88 radian while the corresponding reactive power is Q = 978 VAR. These two powers are carried theoretically by the fundamental currents, from where the apparent power carried by these currents which will have to be of the order of $\mathbf{(P_{gpv}^2+Q^2)^{1/2}}$ = 2.048 VA.

The GPV current obtained during the simulation for a command θ_{Vcom} = -0.88 radian corresponding is Ip = 3.4 A for an stabilized operating regime. This current corresponds to the average value of the DC current switched by the inverter. We will have respectively for the current of a phase of the inverter the effective value (I_{eff}) and the fundamental one (I_F) of current which follow: I_{eff} = 2,8 A and I_{Feff} = 2,7 A. Because, that we have a simple mains voltage: V_{eff} = 256 V, the apparent power delivered by the inverter is S = 2.150 VA. The power carried by the fundamentals of these currents is P_F = 2.074 VA. So we can see that we $\mathbf{P_F = (P_{gpv}^2+Q^2)^{1/2}}$ to about 1.3%. We can deduce that the deforming power generated by the current inverter will be of the form:

$D = (S^2-P_F^2)^{1/2}$

then $D = (S^2-P_{gpv}^2-P_F^2)^{1/2}$

hence D = 567VA.

5. Conclusions

In this article we presented the injection of photovoltaic solar energy into the electricity grid by a static switch. The simulation results show the power control capability of the inverter to effectively control the operating point of the GPV, thus optimally transferring the available energy for a given temperature and sunshine. The results obtained in this article are based on the temporal and spectral analysis of the currents of the inverter. These pre-compensation line currents are currents which have a harmonic richness such that one reaches rates of distortion (THD) of 30%. This will require the implementation of a harmonic compensator. We also highlighted the reactive energy consumption by the inverter.

Acknowledgments

I thank you for finishing this work. My goal and my country can get out of the problem of energy deprivation that it lives until now. I am studying so that in the end I can have long-term solutions to get out of this great scourge. This demand for reactive energy depends of the command of the inverter. If it is desired to impose on the sector level a unit power factor operation, in addition to the harmonic compensation, it will also be necessary to implement a reactive energy compensator.

References

[1] Nassar-eddine I, Obbadi A, Errami Y, El fajri A, Agunaou M. « Parameter estimation of photovoltaic modules using iterative method and the Lambert W function: a comparative study», Energy Convers Manage 2016; 119:37–48.

[2] Soteris A. Kalogirou « Appendix D - Global photovoltaic Markets», McEvoy's Handbook of Photovoltaics (Third Edition) , Academic Press, 2018,Pages 1231-1235.

[3] Lixin Tian, Jianglai Pan, Ruijin Du, Wenchao Li, Zaili Zhen, Gao Qibing, «The valuation of photovoltaic power generation under carbon market linkage based on real options, Applied Energy »,Applied Energy,Volume 201, 2017, Pages 354-362.

[4] E. Płaczek-Popko, « Top PV market solar cells 2016», Opto-Electronics Review, Volume 25, Issue 2, 2017,Pages 55-64.

[5] Maria Malvoni, Maria Grazia De Giorgi, Paolo Maria Congedo « Study of degradation of a grid connected photovoltaic system » Energy Procedia, Volume 126, 2017, Pages 644-650.

[6] Arash Anzalchi, Arif Sarwat « Overview of technical specifications for grid-connected photovoltaic systems», Energy Conversion and Management, Volume 152, 2017, Pages 312-327.

[7] S. Ben Mabrouk, H. Oueslati, A. Ben Mabrouk, G. Zizzo, F. Massaro « Simulation of photovoltaic installation connected to the grid with storage system», Energy Procedia,Volume 139,2017, Pages 609-

616.

[8] S. Kann, M.J. Shiao, C. Honeyman, N. Litvak, J. Jones, L. Cooper, T. Kimbis, J. Baca, S. Rumery, A. Holm, U.S. Solar Market Insight Report |Q3 2015| Executive Summary, U.S. Solar Energy Industry Association (SEIA) and Greentech Media Company (GTM) Research, 2015.

[9] S. Kann, M.J. Shiao, C.Honeyman, N. Litvak, J. Jones, L. Cooper, T. Kimbis, J. Baca, S. Rumery, A. Holm, U.S. Solar Market Insight Report |Q2 2012| Executive Summary. U.S. Solar Energy, 2012.

[10] D'Adamo I, Rosa P. Current state of renewable energies performances in the European Union: a new reference framework. Energy Convers Manage 2016; 121:84–92.

[11] International Energy Agency. 2DS-hiRen Scenario, Energy Technology Perspectives; 2012.

[12] Arif MS. Residential solar panels and their impact on the reduction of carbon emissions. Reduction of carbon emissions using residential solar panels. ⟨https:// www.nature.berkeley.edu/classes/es196/projects/2013final/ArifM_2013.pdf⟩ [Accessed 09/02/ 2018]; 2013.